Rubber-Modified Epoxies. II. Influence of the Cure Schedule and Rubber Concentration on the Generated Morphology

D. VERCHERE,[1] J. P. PASCAULT,*[,1] H. SAUTEREAU,[1] S. M. MOSCHIAR,[2] C. C. RICCARDI,[2] and R. J. J. WILLIAMS[2]

[1]Laboratoire des Matériaux Macromoléculaires, URA CNRS no. 507–Institut National des Sciences Appliquées, 20 Avenue A. Einstein, 69621 Villeurbanne Cedex, France, and [2]Institute of Materials Science and Technology (INTEMA), University of Mar del Plata and National Research Council (CONICET), 7600 Mar del Plata, Argentina

SYNOPSIS

The morphology of a system consisting of a bisphenol A diglycidylether (DGEBA) based epoxy, cured with a cycloaliphatic diamine (4,4′-diamino-3,3′-dimethyldicyclohexylmethane, 3DCM), in the presence of an epoxy-terminated butadiene-acrylonitrile random copolymer (ETBN), was studied as a function of the cure schedule and the initial rubber concentration. Scanning (SEM) and transmission (TEM) electron microscopy, differential scanning calorimetry (DSC) and dynamic mechanical analysis were used to characterize the generated morphology. SEM results were not affected by the type of mechanical test and strain rate. Trends observed for the particle size distribution, the volume fraction of dispersed phase, the concentration of dispersed phase particles and the composition of both phases as a function of polymerization temperature and rubber concentration, were discussed. A correlation between the viscosity at the cloud point and the average size of dispersed phase particles was found for different systems, independently of the cure temperature and the initial rubber amount.

INTRODUCTION

In the context of a cooperation program between our laboratories, a particular rubber-modified epoxy was carefully studied to get a deep understanding of the different factors affecting the phase-separation process, the resulting morphologies, and mechanical properties. The particular system consists of a bisphenol A diglycidylether (DGEBA) based epoxy cured with a cycloaliphatic diamine (4,4′-diamino-3,3′-dimethyldicyclohexylmethane, 3DCM), in the presence of an epoxy-terminated butadiene–acrylonitrile random copolymer (ETBN). In the first part of this series the influence of ETBN on the polymerization and phase-separation processes were reported.[1] The aim of this second part is to analyze the influence of the cure schedule and initial rubber concentration on the generated morphologies. Following parts will deal with the analysis of experimental trends in terms of a phase-separation model, and with the correlation of mechanical properties with morphologies.

Several authors have previously analyzed the influence of cure schedule and rubber amount on resulting morphologies.[2-12] The cure cycle is based on the fact that morphology development is arrested at gelation (in fact well before gelation), for practical purposes. It is, therefore, only necessary to gel at a prescribed temperature to develop the intended morphology. The system may then be cured at a second higher temperature to attain the maximum glass transition temperature (T_g). Analysis of experimental results shows that the concentration of dispersed-phase particles decreases as temperature increases[4,5,10,12]; the volume fraction of dispersed phase remains practically constant,[7,10,12] goes through a maximum[4] or decreases,[4,5] as temperature increases, and the average diameter of dispersed-phase particles goes through a maximum[4,10] or increases,[7,12] as temperature increases. Regarding the influence of initial rubber concentration, everyone agrees that increasing the rubber amount leads to

* To whom correspondence should be addressed.

Journal of Applied Polymer Science, Vol. 42, 701-716 (1991)
 CCC 0021-8995/91/030701-16$04.00

higher values of volume fraction and average diameter of dispersed-phase particles.[2,3,6-9,11,12]

Differences in reported trends may be due to several factors such as the relative values of phase separation and polymerization rates,[4,13] and changes in the characteristics of networks produced at different temperatures with specific curing agents such as piperidine, tertiary amines, or dicyandiamide.

An interesting experimental observation reported in a previous paper,[12] is the fact that the average particle size of dispersed domains, $\bar{D}$, could be correlated with the viscosity of the system at the cloud point, η_{cp}. A straight line of negative slope was obtained when representing ln η_{cp} vs. $\bar{D}$. As η_{cp} decreases when temperature increases, the correlation reflects the observed increase of $\bar{D}$ with precure temperature. This system was based on a DGEBA-type epoxy cure with 1,8 *p*-menthane diamine (MNDA), in the presence of an epoxy-terminated butadiene–acrylonitrile random copolymer (ETBN). One of our purposes here is to check the validity of this correlation for the system based on 3DCM as hardener. Results for two different types of ETBNs will be reported.

Two main techniques are normally used for characterization of morphologies: scanning electron microscopy (SEM) and transmission electron microscopy (TEM). Both will be used to characterize the resulting morphologies. Moreover, differential scanning calorimetry (DSC) and dynamic mechanical analysis (DMA) will be used to reveal features that are not observed by electron microscopy.

EXPERIMENTAL

Materials

The chemical structures and characteristics of the different reagents are shown in Figure 1. The DGEBA-based epoxy was DER 332 (Dow), with an equivalent weight of epoxy groups equal to 174.3 g/eq ($\bar{n}$ = 0.03). The diamine was 4,4′-diamino-3,3′-dimethyldicyclohexylmethane (3DCM, Laromin C260, BASF). The CTBN rubber was Hycar 1300 × 8 (Goodrich), with a number average molecular weight close to 3600, a 18% acrylonitrile content (AN %) and a COOH functionality equal to 1.8. This is the rubber that will be referred to in what follows unless otherwise stated. For comparison purposes two other rubbers, one, CTBN × 9, differing in the COOH functionality, equal to 2.3, and the other, CTBN × 13, differing in the AN %, equal to 26%, will be also used.

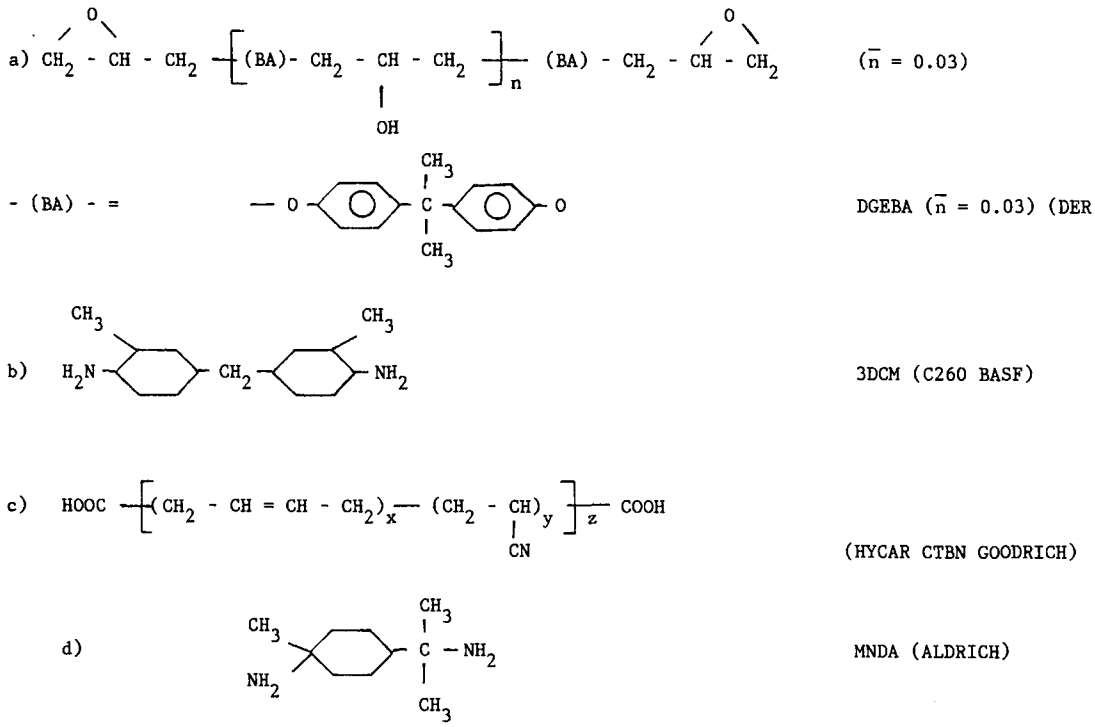

Figure 1 Structural formulae of epoxy prepolymer, diamines, and CTBN rubbers.

ETBN adducts with the DGEBA ($\bar{n} = 0.03$) were prepared following a procedure previously described.[8] It essentially consists of an almost complete reaction of carboxyl groups with epoxides, using a carboxyl-to-epoxy ratio equal to 0.065, at 85°C, in the presence of 0.18% by weight of triphenylphosphine. Due to the large excess of DGEBA, most of the ETBN is a solution of a triblock copolymer (DGEBA/CTBN/DGEBA) in the epoxy monomer.

The structure of a different diamine (1,8 *p*-menthane diamine, MNDA) is also shown in Figure 1. Results obtained with the use of this hardener to cure a DGEBA-based epoxy ($\bar{n} = 0.15$), have been previously reported.[12] They will be used here for comparison purposes.

Formulations and Cure Cycles

The formulations were prepared by incorporating the selected amount of ETBN to the epoxy monomer, stirring under vacuum at moderate temperatures, cooling to room temperature, and mixing with a stoichiometric proportion of diamine (with respect to the sum of epoxides coming from monomer and adduct). The CTBN rubber concentration in the formulation will be expressed as a percentage of mass fraction, % R, or as a volume fraction, ϕ_R. Four different levels of initial rubber concentration were selected, % R = 6.5, 10.6, 15, and 20.

In order to prepare specimens for morphological characterization, formulations were cast into a PTFE-coated aluminum mold (200 × 200 × 6 mm), and precured at a temperature T_i during a time necessary to arrest the phase separation by gelation.[1] Four different precure temperatures were selected: 29, 50, 75, and 100°C. Corresponding precure times were: 6 days, 360–400 min, 90–120 min, and 50 min, respectively. Samples were postcured for 14 h at 190°C to get the maximum conversion of the epoxy–diamine matrix, without any degradation reactions.[1,14]

Scanning Electron Microscopy (SEM)

Different ways of producing the fracture surface were compared. They include tensile, flexural, and impact tests at room temperature. Tensile tests were performed at a strain rate of 3×10^{-4} s^{-1}. Flexural tests were carried out using a single-edge-notched (SEN) specimen, in a three-point bending mode, at a strain rate of 5.2×10^{-4} s^{-1}.[15] The Charpy impact test was performed on unnotched specimens, using a three-point bending feature (distance between supports equal to 40 mm), at a strain rate of 112 s^{-1}.[15]

Fracture surfaces were observed using a scanning electron microscope JEOL 840 A, after coating with a gold sputterer. The detection level was close to 0.1 μm.

Figure 2(a) shows the crack trajectory going through the equatorial planes of particles that is observed in SEM micrographs.[10] This leads to an estimation of higher volume fractions and concentrations of dispersed phase particles that are actually present. In fact, what is measured is the effective volume fraction of particles for crack propagation. Distances between centers, d_c, and surfaces, d_p, are assigned lower values than actual ones, as shown in Figure 2(a).

Micrographs were magnified to calculate morphological parameters. The region under analysis contained about one hundred particles of dispersed phase. The distribution of diameters was determined by measuring individual areas using a HP9111 A graphic integrator associated with a HP85 calculator. Therefore, the raw data gave us the number of particles per unit surface, $\bar{N}$ (SEM) (part/μm^2),

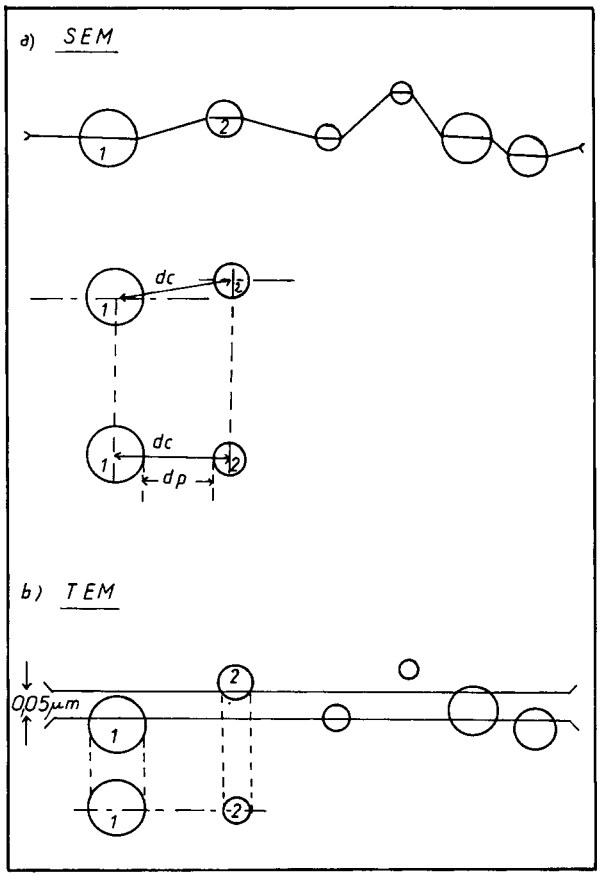

Figure 2 Difference in possible crack trajectories (a) on equatorial planes and (SEM) (b) randomly (TEM).

and the particle size distribution, n (number of particles having a diameter D) vs. D. Also, by taking several particles at random, the average distances among centers, $\overline{d_c}$, and surfaces $\overline{d_p}$, were determined. From this information the following parameters were calculated:

i) Average diameter of particles

$$\bar{D}\,(\mathrm{SEM}) = \frac{\sum nD}{\sum n} \tag{1}$$

ii) Volume fraction of dispersed phase: An effective volume fraction of dispersed phase may be calculated as[10]

$$V_D\,(\mathrm{SEM}) = (\pi/4) \sum nD^2/A_T \tag{2}$$

where A_T is the area of the micrograph region under analysis. Equation (2) assumes that the volume fraction is an isotropic property, hence, values measured in the plane are the same as in the volume. This volume fraction is regarded as an effective value because it is measured in the plane where the crack propagation has taken place [Fig. 2(a)].

A different way to calculate the volume fraction of dispersed phase has been proposed.[12] It assumes that the "rugosity" of the crack propagation plane has a height equal to $\bar{D}$. Then, the volume of the region where the particles are being counted is $A_T \times \bar{D}$. Therefore, it is proposed that

$$V(\bar{N}, \bar{D}) = \frac{\bar{N}\,(\mathrm{SEM})}{\bar{D}} \times (\pi/6)\,\bar{D}^3 = (\pi/6)\,\bar{N}\,(\mathrm{SEM})\,\bar{D}^2 \tag{3}$$

Both volume fractions are related by

$$V(\bar{N}, \bar{D}) = \frac{2}{3} \times V_D\,(\mathrm{SEM}) \times \frac{\bar{D}^2}{\overline{D^2}} \tag{4}$$

iii) Concentration of dispersed phase particles

$$P\,(\mathrm{SEM}) = \frac{\text{number of particles}}{\text{total volume}} = \frac{V_D\,(\mathrm{SEM})}{(\pi/6)(\sum nD^3)} \times \sum n \tag{5}$$

In terms of the assignation of a "rugosity" equal to $\bar{D}$ to the crack propagation plane, the concentration of dispersed phase particles is simply calculated as

$$P(\bar{N}, \bar{D}) = \frac{\bar{N}(\mathrm{SEM})}{\bar{D}} \tag{6}$$

Transmission Electron Microscopy (TEM)

Transmission electron micrographs were obtained from specimens that had been stained with ruthenium chloride and microtomed at room temperature to give a thickness of 500 Å (0.05 μm). A Philipps EM301 was used, at magnifications of ×20,800, ×28,800, and ×44,800.

Figure 2(b) shows how microtoming gives a random cut of dispersed phase particles.[10] If the size distribution lies in a region of diameters higher than the section thickness (0.05 μm), one would expect to determine correct values for the volume fraction of dispersed phase, V_D (TEM) and number of particles per unit surface, $\bar{N}$ (TEM) (part/μm^2). The particle size distribution n vs. $\bar{D}$ was determined in the same way as in the SEM technique. Then, the following parameters were calculated:

i) Average diameter of particles

$$\bar{D}(\mathrm{TEM}) = \frac{\sum nD}{n} \tag{7}$$

ii) Volume fraction of dispersed phase

$$V_D\,(\mathrm{TEM}) = (\pi/4)\,\frac{\sum nD^2}{A_T} \tag{8}$$

The value arising from eq. (8) was compared with the one obtained by tracing a series of parallel lines on the micrograph, at intervals of 0.1 μm, and determining the fraction of each line corresponding to dispersed phase particles.

iii) Concentration of dispersed phase particles: Assuming that SEM gives the correct particle size distribution while TEM gives the correct value for the volume fraction of dispersed phase, the concentration of dispersed phase particles may be calculated as

$$P\,(\mathrm{STEM}) = \frac{V_D\,(\mathrm{TEM})}{(\pi/6)[\sum nD^3/\sum n]\,(\mathrm{SEM})} = \frac{V_D\,(\mathrm{TEM})}{V_D\,(\mathrm{SEM})} \times P\,(\mathrm{SEM}) \tag{9}$$

Glass Transition Temperatures (T_g)

The glass transition temperature of the continuous phase (epoxy–diamine matrix containing some dissolved rubber even after phase separation), was determined by DSC (Mettler TA 3000), at a 10°C/min heating rate, under argon atmosphere (value determined at the onset of the transition). The T_g of the dispersed phase (rubber-rich) was also determined by DSC, in the same conditions, but using an unmodified epoxy–diamine matrix as a reference, as proposed by Kunz et al.[6] This method was satisfactory for samples containing 10.6% R or more.

Relaxations of both phases were determined from dynamic mechanical measurements. A Rheometrics dynamic analyzer was used at an oscillation frequency of 0.016 Hz. As the α relaxation associated to the glass transition of the rubbery phase is close to the β relaxation of the epoxy network (associated to motions of hydroxyether and diphenylpropane groups[16]), it was necessary to operate at a very low frequency to separate both relaxations.[17] A deconvolution technique enabled us to obtain the α relaxation of the rubbery phase.

MORPHOLOGIES

Influence of the Fracture Mode on SEM Results

Fracture surfaces produced by tensile, flexural, and impact tests, for samples containing 15% R and precured at 100°C, were analyzed by SEM. Results are shown in Table I. Within the range of experimental error it may be concluded that morphological parameters determined by SEM are not affected by the type of fracture mode (mechanical solicitation and strain rate). Another conclusion from this comparison is the reproducibility of SEM results for different samples of the same formulation and precure temperature. In order to visualize the resulting morphology, Figure 3 shows SEMs of samples containing 15% R and precured at different temperatures. An apparent unimodal distribution is observed for every case, with diameters lesser than 1 μm.

Comparison of SEM and TEM Results

Table II shows a comparison of morphological parameters obtained using SEM and TEM techniques for samples containing different rubber amounts and precured at several temperatures.

The average diameters measured by SEM are always higher than the corresponding values determined by TEM. As discussed in the experimental section this was an expected result because of the way in which the fracture surface is produced. SEM gives correct values while TEM gives apparent values due to the random cut of the spheres. Although it is possible to obtain the true frequency distribution of particle sizes from the apparent distribution observed in TEM by solving an Abel-type integral equation[6] it is better to get it directly using the SEM technique. In fact, many of the values of average diameters reported in the literature are apparent values obtained by TEM. By assuming that the TEM distributions arise from spherical particles cut at random, the true average diameters may be obtained by multiplying the apparent average diameter by $4/\pi$, as arises from statistical calculations.[18–20] Table II shows that this is, in fact, what happens, within the experimental error. In what follows, the particle size distribution obtained by SEM will be only considered.

Table I Influence of the Fracture Mode at 25°C on Morphological Parameters Determined by SEM, for a Sample Containing 15% R, Precured at 100°C (σ = Standard Deviation)

Type of Test	$\bar{D}$ (SEM) (μm)	$\overline{dc}$ (μm)	$\overline{dp}$ (μm)	$\bar{N}$ (SEM (part/μm^2)
Impact (Charpy) $\dot{\epsilon} = 112\ s^{-1}$ (15)	0.465 (σ = 0.09)	0.96	0.49	1.21
Tensile $\dot{\epsilon} = 3 \times 10^{-4}\ s^{-1}$	0.46 (σ = 0.127)	1.05	0.59	1.23
Flexural (3 p. bending) $\dot{\epsilon} = 5.2 \times 10^{-4}\ s^{-1}$ (15)	0.46 (σ = 0.09)	1.00	0.60	1.21

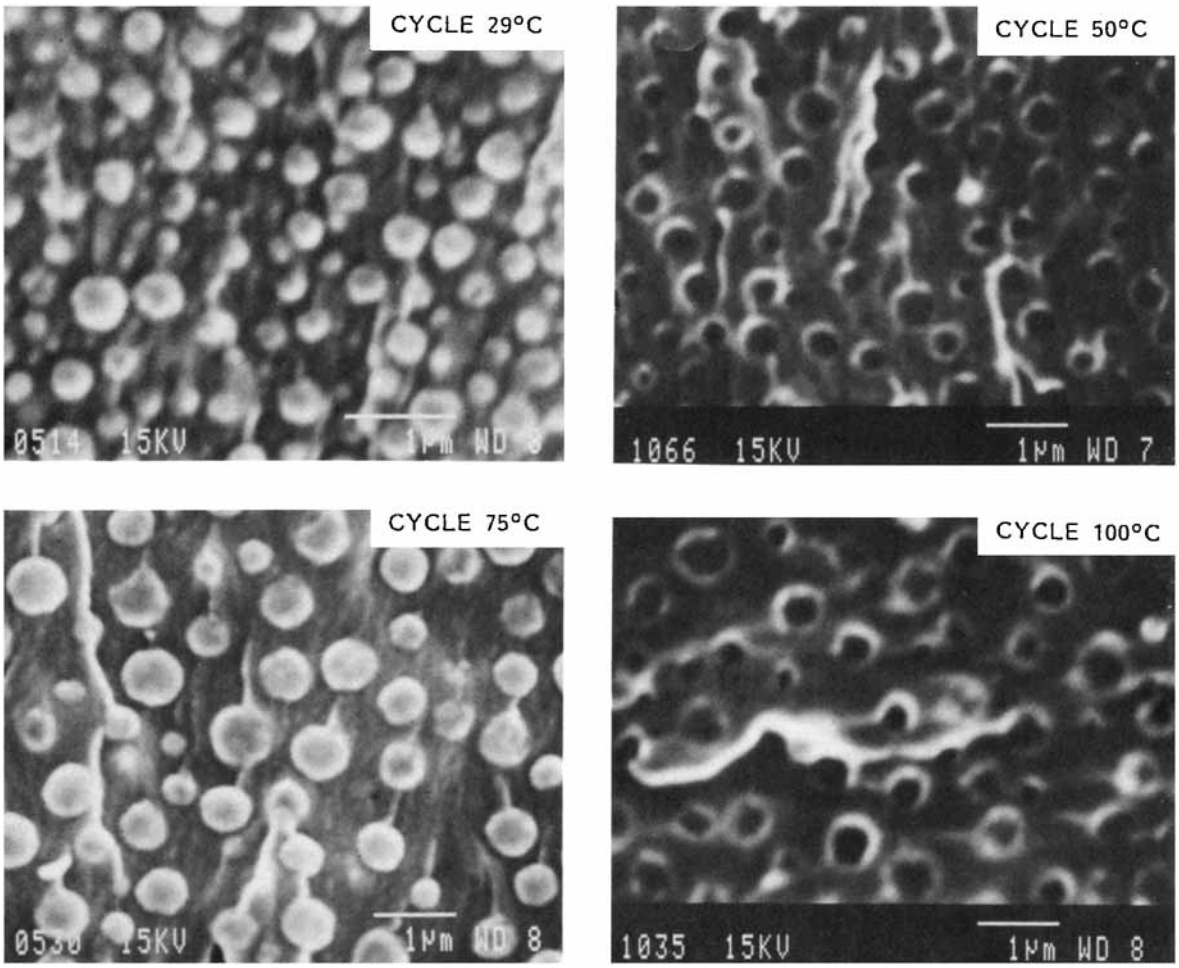

Figure 3 SEMs of samples containing 15% R, precured at T_i = 29°C (I), 50°C (II), 75°C (III), and 100°C (IV). The arrow indicates the direction of crack propagation.

The average distances center-to-center, $\overline{d_c}$, and surface-to-surface, $\overline{d_p}$, of dispersed phase particles are also shown in Table II. These values were obtained from SEM micrographs as indicated in the experimental section.

The comparison between the number of particles per unit surface arising from SEM and TEM techniques is presented in Table II. Contrary to the case of the average diameter, no definite trend in the values arising from both techniques is observed, i.e., depending on the particular sample, TEM gives higher or lower values than SEM. Possibly this difference is merely a consequence of the range of experimental uncertainty. In turn, this has a direct influence on the volume fraction and concentration of dispersed phase particles that are calculated from both techniques (Table II).

Due to the uncertainty in the best set of morphological parameters, and the fact that the particle size distribution has to be obtained from SEM micrographs, in what follows, the discussion will be limited to the analysis of SEM results, taking the effective volume fraction of dispersed phase, V_D (SEM), as the value for comparison purposes. Moreover, it will be shown that the use of some of the volume fractions arising by TEM does not satisfy mass balances in the system. This means that V_D (TEM) can not be taken as a correct value, at least for every case.

Regarding $V(\bar{N}, \bar{D})$ values shown in Table II, they confirm that the thickness of SEM micrographs is close to $\bar{D}$.

Particle Size Distribution

Figure 4(a) shows particle size distributions for samples containing 15% R and precured at several temperatures, T_i = 29°C, 50°C, 75°C, and 100°C. For comparison purposes distributions previously reported,[12] found by using a different diamine

Table II Morphological Parameters Obtained Using SEM and TEM Techniques for Samples Containing Different Rubber Amounts and Precured at Several Temperatures (σ = Standard Deviation)

% R	6.5		10.6		15				20
T_i (°C)	50	75	50	75	29	50	75	100	75
$\bar{D}$ (SEM), μm	0.26	0.36	0.31	0.37	0.27	0.35	0.43	0.46	0.55
(σ)	(0.09)	(0.074)	(0.095)	(0.091)	(0.08)	(0.09)	(0.14)	(0.10)	(0.15)
$\bar{D}$ (TEM), μm	0.16	0.23	0.25	0.28	0.22	0.25	0.34	0.35	0.48
(σ)	(0.05)	(0.05)	(0.06)		(0.07)	(0.10)	(0.10)	(0.09)	(0.11)
$\frac{4}{\pi}\bar{D}$ (TEM), μm	0.20	0.29	0.32	0.36	0.28	0.32	0.43	0.45	0.61
$\overline{dc}$, μm	1.12	1.20	1.02	0.99	0.48	0.75	0.97	1.08	1.02
$\overline{dp}$, μm	0.78	0.81	0.63	0.59	0.20	0.41	0.54	0.65	0.46
$\bar{N}$ (SEM), part/μm^2	1.80	0.83	1.50	1.48	4.65	2.30	1.60	1.21	1.10
$\bar{N}$ (TEM), part/μm^2	2.3	1.4	2.3	1.3	5.0	2.3	1.4	1.6	1.3
V_D (SEM)	0.107	0.089	0.132	0.172	0.297	0.254	0.248	0.220	0.29
$V(\bar{N}, \bar{D})$	0.064	0.056	0.075	0.106	0.177	0.147	0.155	0.134	0.174
V_D (TEM)	0.047	0.061	0.118	0.090	0.210	0.136	0.140	0.160	0.245
P (SEM) $\times 10^{-12}$ part/cm^3	8.7	3.2	6.4	5.4	23	9.3	4.6	3.9	2.7
$P(\bar{N}, \bar{D}) \times 10^{-12}$ part/cm^3	6.9	2.3	4.8	4.0	17	6.5	3.7	2.6	2.0
P (STEM) $\times 10^{-12}$ part/cm^3	3.8	2.2	5.7	2.8	16	5.0	2.6	2.8	2.3

(MNDA), are shown in Figure 4(b). It is seen that in both cases the average diameter increases with polymerization temperature. However, in the present case the selected diamine (3DCM) gives smaller particles than those obtained with the use of MNDA. Average particle sizes have been reported in the range of 1.8–4 μm when using 4,4′-diaminodiphenyl methane[6] and 1.7–3.5 μm with dicyandiamide.[8] These ranges of particle sizes are higher than those observed with MNDA, 0.7–1.6 μm, or 3DCM, 0.2–0.6 μm. Therefore, the nature of the diamine has a significant influence on the resulting morphologies.

Figure 5 shows the increase in the average particle size as a function of precure temperature for different systems: (a) is the system under study, (b) is the same system but with the use of ETBN × 9 instead of ETBN × 8, and (c) is the system with MNDA instead of 3DCM. Every case shows the same influence of precure temperature on average particle size, and the same occurs for different rubber concentrations (Table II). As stated in the introduction previous reported results showed either the same trend as here,[7,12] or the presence of a maximum.[4,10] This maximum is observed when the precure temperature is so high that the volume fraction of dispersed phase shows a considerable drop after the maximum. In this case phase separation is controlled by the polymerization rate, i.e., the polymer gels so rapidly that phase separation is severely limited.[4,13] Therefore, the trend reported here for every system must be associated to the fact that polymerization rates are very much slower than phase separation rates. This type of behavior has been predicted by using a phase separation model.[13]

The influence of the initial rubber concentration on the resulting particle size distributions is shown in Figure 6, for samples precured at 50°C. Increasing the rubber amount leads to an increase in the average size of dispersed phase particles. This agrees with most of the experimental results previously reported.[3,6–9,11,12] A similar trend is observed in Table II for a precure temperature of 75°C.

Particle size distributions were also measured during polymerization, for samples precured at 50°C.

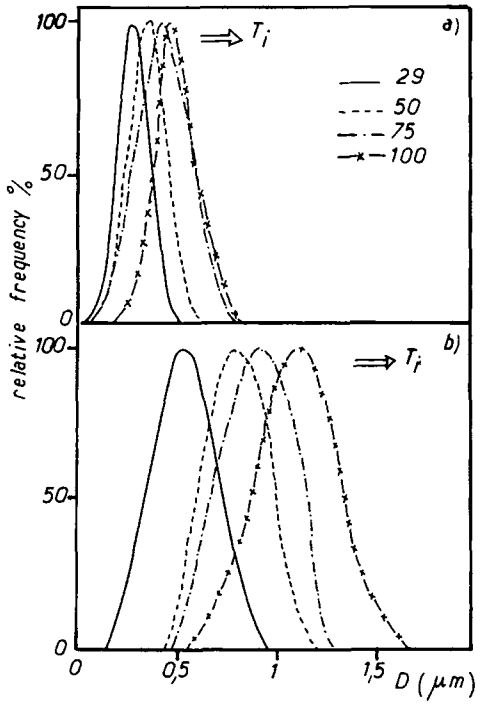

Figure 4 Particle size distributions at different precure temperatures (a) 3DCM-DGEBA ($\bar{n}$ = 0.03)—15% R and (b) MNDA-DGEBA ($\bar{n}$ = 0.15)—15% R.

Figure 7 shows the evolution of the average particle diameter after polymerization times such that the T_g of the sample is higher than room temperature (after 3 h at 50°C, T_g = 26°C). This last condition is necessary for the metalization of the surface. Also shown in the figure are the times at the beginning (t_{cp}) and end ($t_{cp+\Delta cp}$) of phase separation, vitrification time (t_{vit}) and gelation time (t_{gel}). The corresponding conversions are shown on another scale.[1] Clearly, the final morphology is attained well before gelation or vitrification as was discussed in the first part of the series.[1] The point corresponding to $\bar{D}$ = 0.1 μm just indicates the detection limit of the cloud-point device.[1] From the experimental value of $t_{cp+\Delta cp}$ it seems that the final morphology is produced in a very narrow conversion range. The postcure step has no effect on the morphology.

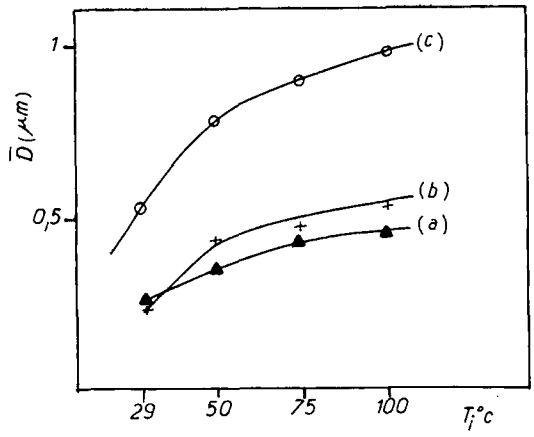

Figure 5 Average particle size as a function of precure temperature for different systems (a) DGEBA ($\bar{n}$ = 0.03)–3DCM—15% R8; (b) DGEBA ($\bar{n}$ = 0.03)–3DCM—15% R9; (c) DGEBA ($\bar{n}$ = 0.15)–MNDA—15% R8.

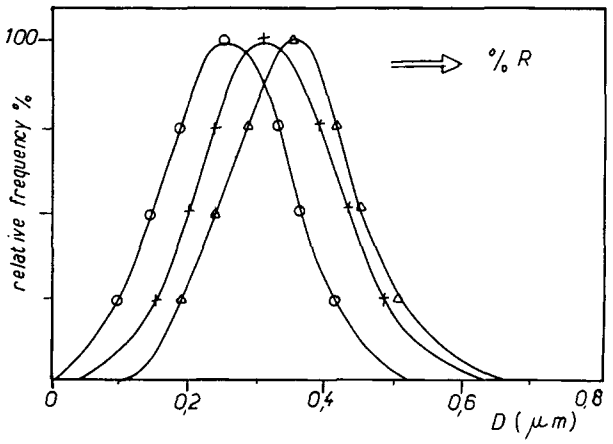

Figure 6 Influence of the initial rubber concentration (% R) on particle size distributions for samples precured at 50°C: (○) 6.5% R; (+) 10.6% R; (△) 15% R.

Effective Volume Fraction of Dispersed Phase

Figure 8 shows the effective volume fraction of dispersed phase, V_D (SEM), as a function of the precure temperature for samples containing different initial rubber amounts. Within the range of experimental error it may be ascertained that the volume

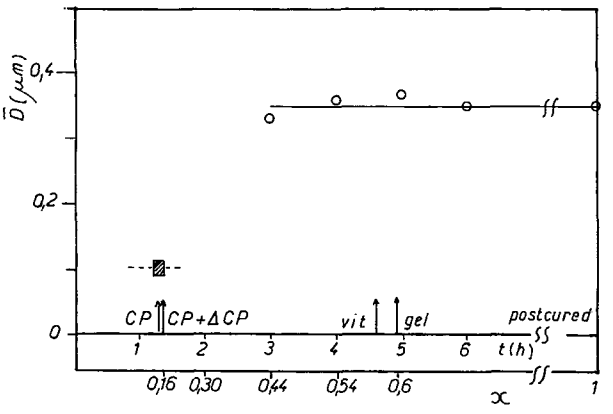

Figure 7 Evolution of the average particle diameter during the cure at 50°C for a system containing 15% R.

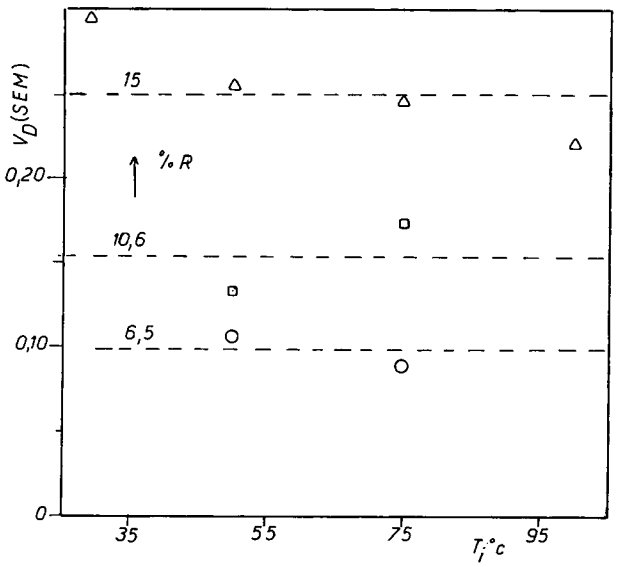

Figure 8 Effective volume fraction of dispersed phase, V_D (SEM), as a function of the precure temperature, T_i (°C), for samples containing different initial rubber amounts.

fraction of dispersed phase increases significantly with the initial rubber concentration but does not depend very much on the precure temperature. The constancy of the volume fraction of dispersed phase with polymerization temperature has been observed for different systems,[7,10,12] and may be explained through the fact that polymerization rate does not control the phase separation rate.[13] Otherwise, a decrease of V_D with increasing temperature will be observed.[4,5] The increase of the volume fraction of dispersed phase with the initial rubber amount has always been reported.[2,3,6-8,11,12]

Concentration of Dispersed Phase Particles

As shown in Table II, the concentration of dispersed phase particles, P (SEM), decreases with an increase in the precure temperature and does not show a significant variation with the initial rubber amount. The decrease in the concentration of particles when increasing polymerization temperature has been reported by several authors,[4,5,10,12] and it is expected whether polymerization rate controls phase separation or not.[13]

As previously discussed, in the region where the rate of phase separation determines the morphology (as is the case here), the volume fraction of dispersed phase does not vary significantly with cure temperature. Then, the decrease in the concentration of dispersed phase particles associated with a constant volume fraction of dispersed phase implies that the average size of particles must increase with temperature, as is actually observed.

Ratio of Morphological Parameters Associated with Mechanical Behavior

Although the influence of generated morphologies on mechanical properties will be discussed in another part of this series, it is interesting to compare morphologies of different samples with respect to criteria related to the mechanical behavior. For example, Table III shows the ratio of the average particle size with respect to the average surface-to-surface distance, $\bar{D}/\overline{d_p}$, for different formulations and precure temperatures. We may expect to have an increase in toughness with the value of $\bar{D}/\overline{d_p}$ because of the interconnection of stress fields. Thus, the increase in the initial rubber concentration will be useful for this purpose (a simultaneous decrease of the T_g of the matrix, by the dissolved rubber remaining after phase separation, will act, in the same sense, by the enhancement of the ability of the matrix to undergo plastic deformation[21]). For a 15% R in the initial formulation, a lower precure temperature seems to be better as it gives a higher value of the ratio.

Table III Ratio of Morphological Parameters Associated With Mechanical Behavior for Samples Containing Different Rubber Amounts and Precured at Several Temperatures

	6.5% R		10.6% R		15% R				20% R
	T_i = 50°C	T_i = 75°C	T_i = 50°C	T_i = 75°C	T_i = 29°C	T_i = 50°C	T_i = 75°C	T_i = 100°C	T_i = 75°C
$\bar{D}/\overline{dp}$, SEM	0.33	0.44	0.49	0.63	1.35	0.85	0.80	0.71	1.20
$\frac{V_D^2\ (\text{SEM})}{\bar{D}\ (\text{SEM})}$, μm^{-1}	0.044	0.022	0.056	0.080	0.327	0.184	0.143	0.105	0.153

Recently, Sjoerdsma[22] proposed a new criterion for the critical value characterizing the transition from brittle to tough behavior. In the range of $\bar{D}$ going from 0.4 μm to 3.6 μm, and from data of Wu,[23] it was found that

$$V_D^2/\bar{D} > 0.034 - 0.057\ \mu m^{-1},$$

to attain a tough behavior. From values of Table III it may be inferred that a 6.5% R may not be enough to toughen the network.

COMPOSITION OF PHASES

Composition of the Continuous Phase

Values of the T_g of the epoxy network, ${}_ET_g$, are shown in Table IV, for samples containing different initial rubber amounts and precured at several temperatures. Samples were always postcured at 190°C to achieve the maximum T_g. The T_g of the matrix without rubber is[14]: ${}_ET_{g\,\text{pure}} = 180°C$, while the glass transition temperature of the pure rubber (CTBNx8), measured by DSC at the same scanning rate, is[1]: ${}_RT_{g,\text{pure}} = -60°C$.

As values of ${}_ET_g$ reported in Table IV are lower than ${}_ET_{g,\,\text{pure}}$, some of the rubber must remain as a solution in the matrix at the end of the cure. The volume fraction of rubber dissolved in the matrix may be calculated by assuming the validity of Fox equation[1,24]

$$\frac{1}{{}_ET_g} = \frac{(1 - W_R^C)}{{}_ET_{g,\,\text{pure}}} + \frac{W_R^C}{{}_RT_{g,\,\text{pure}}} \tag{10}$$

By taking the ${}_ET_g$ values reported in Table IV, the mass fraction of rubber dissolved in the matrix, W_R^C, may be obtained. These are in turn expressed as volume fractions by

$$\phi_R^C = \frac{W_R^C/\rho_R}{W_R^C/\rho_R + (1 - W_R^C)/\rho_E} \tag{11}$$

where $\rho_R = 0.948\ g/cm^3$ and $\rho_E = 1.127\ g/cm^3$, as previously quoted.[1]

As discussed in the first part of the series,[1] ϕ_R^C values (shown in Table IV) increase with the initial

Table IV Glass Transition Temperatures of the Epoxy Network (${}_ET_g$ Measured by DSC, ${}_ET_\alpha$ Measured by Dynamic Mechanical Analysis), and the Rubber (${}_RT_g$ Measured by DSC, ${}_RT_\alpha$ Measured by Dynamic Mechanical Analysis); Ratio of Parameters Characterizing the Asymmetry of the ${}_ET_\alpha$ Relaxation, $(\sigma_1 - \sigma_2)/\sigma_2$, and Volume Fractions and Compositions of the Dispersed Phase Derived From SEM and TEM Techniques

	6.5% R 7.6		10.6% R 12.3		15% R 17.3				20% R 22.9
ϕ_R^0									
T_i (°C)	50	75	50	75	29	50	75	100	75
${}_ET_g$ (°C)	168	167	163	162	155	154	155	153	151
${}_ET_\alpha$ (°C)	177	—	172	—	168	168	—	167	—
${}_RT_g$ (°C)	—	—	−62	−62	−62	−61	−62	−63	−62
${}_RT_\alpha$ (°C)	−67	—	−65	—	—	−64	—	−63	−62
$(\sigma_1 - \sigma_2)/\sigma_2$	0.57	—	0.5	—	1	1	—	1	—
ϕ_R^C, %	2.9	3.1	4.1	4.3	6.1	6.4	6.1	6.6	7.1
SEM:									
$\underline{V_D}$ (SEM)	0.107	0.089	0.132	0.172	0.297	0.254	0.248	0.220	0.290
ϕ_E^D (%)	52.5	46.0	33.3	49.0	56.1	50.4	48.6	44.7	38.4
$V_D\,\overline{\phi_E^D}$ (%)	5.6	4.1	4.4	8.4	16.7	12.8	12.1	9.8	11.1
$V_D\,\overline{\phi_R^D}$ (%)	5.1	4.8	8.8	8.8	13.0	12.6	12.7	12.2	17.9
TEM:									
$\underline{V_D}$ (TEM)	0.047	0.061	0.118	0.090	0.210	0.136	0.140	0.160	0.245
$\overline{\phi_E^D}$ (%)	−2.9	23.1	26.4	6.8	40.6	13.5	13.9	26.5	28.4
$V_D\,\overline{\phi_E^D}$ (%)	−0.1	1.4	3.1	0.6	8.5	1.8	1.9	4.2	7.0
$V_D\,\phi_R^D$ (%)	4.8	4.7	8.7	8.4	12.5	11.8	12.1	11.8	17.5

rubber concentration but do not depend on cure temperature. This is consistent with the fact that the effective volume fraction of dispersed phase did not show a significant variation with cure temperature.

Composition of the Dispersed Phase

The composition of the dispersed phase may be obtained by stating a mass balance of rubber in the overall system. By calling ϕ_R^O, the initial volume fraction of rubber added to the formulation (values are shown in Table IV),

$$\phi_R^O = \frac{(\%)\, R/\rho_R}{(\%\ R)/\rho_R + (100 - \%\ R)/\rho_E} \qquad (12)$$

it must be verified that

$$\phi_R^O = V_D\overline{\phi_R^D} + (1 - V_D)\phi_R^C \qquad (13)$$

By taking $V_D = V_D$ (SEM), the volume fraction of rubber in the dispersed phase may be obtained. Then,

$$\overline{\phi_E^D} = 1 - \overline{\phi_R^D} \qquad (14)$$

The bars over the compositions of the dispersed phase indicate that they must be regarded as average values, considering that a phase separation may also take place inside dispersed domains as will be discussed in what follows.

Table IV shows that the volume fraction of the epoxy copolymer is close to 50%, without showing significant variations among different samples. However, when V_D is replaced by V_D (TEM), a high dispersion in $\overline{\phi_E^D}$ values results, including one negative value without physical sense (Table IV). Therefore, the volume fractions of dispersed domains arising from TEM must be regarded with caution.

NATURE OF DISPERSED DOMAINS

From a mass balance we have shown that about half of the volume fraction of dispersed domains consists of the epoxy–amine copolymer. But, what is the nature of dispersed domains? Is it a homogeneous solution or does phase segregation take place inside the dispersed particles?

Several authors have reported the presence of unstained regions inside the dispersed phase observed in TEM micrographs,[6,25,26] giving direct evidence of a phase-separation inside dispersed domains. Romanchik et al.[26] observed the presence of a core–shell morphology, with about 10–20% of the total volume consisting of a rubbery shell. Unfortunately, we were not able to reveal a phase separation inside dispersed domains with our staining technique. However, an indirect evidence of phase segregation inside dispersed particles is given by the fact that ${}_RT_g$, obtained by DSC (Table IV), is very close to the T_g of pure rubber. In fact, the experimental value is lower than the one of the pure rubber confirming previous results.[4,26] This is attributed to differences in the coefficients of thermal expansion between the glassy epoxy matrix and the rubber-rich phase. The larger coefficient of thermal expansion of the rubber results in constraint of the rubber domains upon cooling below the T_g of the matrix.[4,26] Supporting this assumption, Romanchik et al.[26] showed that ${}_RT_g$ of the rubber contained in dispersed domains, initially present in their uncured system, decreased when the epoxy matrix was crosslinked.

A question that arises is whether the epoxy copolymer contained in dispersed domains has any

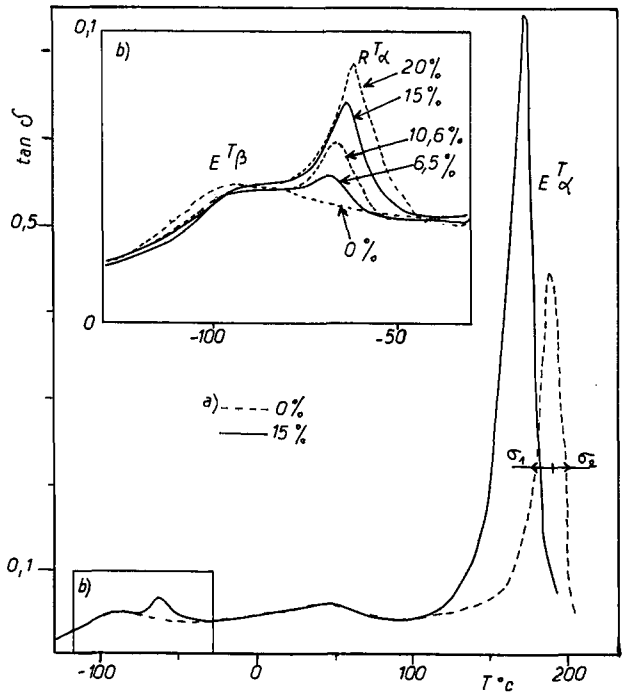

Figure 9 (a) Dynamic mechanical analysis at 0.016 Hz for samples precured at 50°C and containing 0% and 15% R; (b) magnification of the low-temperature region showing ${}_ET_\beta$ and ${}_RT_\alpha$ for samples precured at 50°C and containing 0% (⌓); 6.5% (◇); 10.6% (△); 15% (▲); and 20% R (▽).

measurable difference with respect to the one in the matrix. Using DSC only one relaxation of the epoxy copolymer was found, although it is considered very difficult to observe and quantify interphases with this technique.[27] In order to study this aspect in more detail, dynamic mechanical analysis at a very low frequency (0.016 Hz) was carried out. Figure 9(a) shows a comparison of the relaxations appearing in samples without rubber and containing 15% R (both precured at 50°C). Values of ${}_ET_\alpha$, shown in Table IV, are higher than values of ${}_ET_g$ derived from DSC due to the different ways to take T_g (onset value vs maximum of the peak). The α relaxation of the epoxy copolymer, ${}_ET_\alpha$, shifts to lower temperatures by increasing the initial rubber concentration (Table IV). A significant feature of the ${}_ET_\alpha$ relaxation is that it is not symmetric, i.e., σ_1 and σ_2 measuring the half-widths of the peak at half of its total height [Fig. 9(a)], are not equal. The relative difference $(\sigma_1 - \sigma_2)/\sigma_2$ is 0.17 for the sample devoid of rubber and increases with the initial rubber concentration (Table IV).

Figure 10 shows the correlation betwen the asymmetry of the ${}_ET_\alpha$ relaxation, measured by $(\sigma_1 - \sigma_2)/\sigma_2$, and the overall volume fraction of epoxy polymer in dispersed domains, $V_D\bar{\phi}_E^D$ (Table IV). Then, it may be inferred that the epoxy copolymer present in dispersed domains relaxes in the lower temperature region of the ${}_ET_\alpha$ relaxation. This may be due to the covalently bonded CTBN fragments, and/or to a lower degree of crosslinking of the epoxy copolymer present in dispersed domains because of a nonstoichiometric segregation of epoxy and amine functionalities from the matrix. This last possibility may be related to the slight delay in the gel conversion observed for samples containing 15% R.[1]

The secondary phase separation taking place inside dispersed domains may possibly continue after gelation of the matrix. This would explain the decay in light transmission after gelation observed by Wang and Zupko,[28] and attributed to localized changes in composition.

Regarding the rubber relaxation, ${}_RT_\alpha$, it appears superimposed to the β relaxation of the epoxy ${}_ET_\beta$, as shown in Figure 9. The existence of a qualitative correlation between the intensity of the rubber damping peak in dynamic mechanical analysis and the volume fraction of dispersed phase, has been stated by several authors.[4,21,25] Figure 9(b) shows that the area under the ${}_RT_\alpha$ relaxation increases with the initial rubber concentration. After deconvolution of ${}_ET_\beta$ and ${}_RT_\alpha$ relaxations, the area under the latter may be plotted as a function of the overall volume fraction of rubber in dispersed domains, $V_D\bar{\phi}_R^D$ (Table IV). A very good correlation between both quantities is shown in Figure 10.

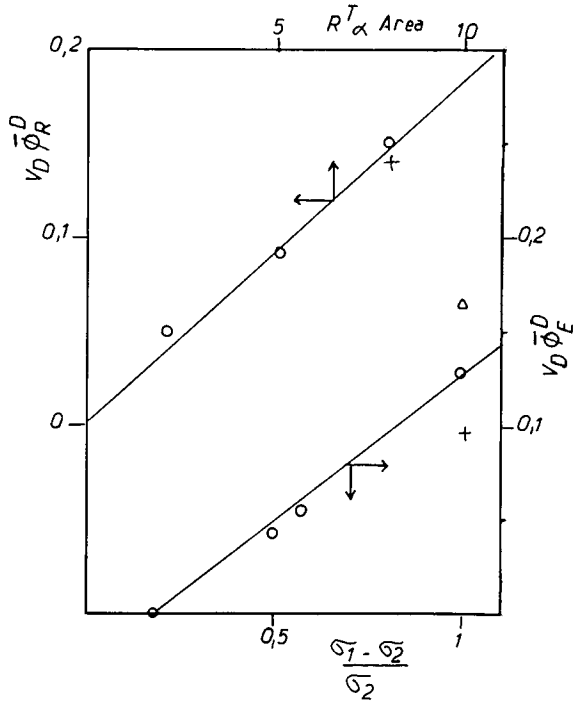

Figure 10 Correlations between the asymmetry of the ${}_ET_\alpha$ relaxation, measured by $(\sigma_1 - \sigma_2)/\sigma_2$, and the overall volume fraction of epoxy polymer in dispersed domains, $V_D\bar{\phi}_E^D$, and between the area under the ${}_RT_\alpha$ relaxation, after deconvolution, and the overall volume fraction of rubber in dispersed domains, $V_D\bar{\phi}_R^D$ [samples precured at 29°C (△); 50°C (○); and 100°C (+)].

We may conclude that there are, in fact, two phases inside the dispersed domains. The rubbery phase relaxes at a lower temperature than pure rubber due to the presence of unrelaxed thermal stresses resulting from differences in the coefficients of expansion on cooling from the cure temperature. The epoxy copolymer relaxes at a temperature very close (not discernible by DSC), but lower (as results from dynamic mechanical analysis), than the matrix. This may be due to the bonds between epoxy and CTBN residues present in dispersed particles and/or to a lower crosslink density of the epoxy copolymer.

AVERAGE SIZE VS. VISCOSITY AT THE CLOUD POINT

It was recently shown[12] that for a DGEBA-based epoxy ($\bar{n} = 0.15$) cured with MNDA in the presence of an epoxy-terminated butadiene–acrylonitrile

Table V Viscosity at the Cloud Point and Average Diameter of Dispersed Phase Particles for Different Systems, Precure Temperatures, T_i, and Initial Rubber Concentrations (σ = Standard Deviation of $\bar{D}$)

System	T_i (°C)	η_{cp} (Pa s)	$\bar{D}$ (μm)	(σ)
DGEBA ($\bar{n}$ = 0.03) 3DCM 6.5% *R*8	50	16	0.26	0.09
	75	2.8	0.36	0.07
DGEBA ($\bar{n}$ = 0.03) 3DCM 10.6% *R*8	50	7.3	0.31	0.09
	75	1	0.37	0.09
DGEBA ($\bar{n}$ = 0.03)	29	66	0.27	0.08
3DCM	50	3	0.35	0.09
15% *R*8	75	0.88	0.43	0.14
	100	0.46	0.46	0.10
DGEBA ($\bar{n}$ = 0.03) 3DCM 20% *R*8	75	2.1	0.55	0.15
DGEBA ($\bar{n}$ = 0.03)	29	938	0.23	0.12
3DCM	50	17.8	0.38	0.12
15% *R*9	75	4.5	0.42	0.10
	100	0.3	0.55	0.11
DGEBA ($\bar{n}$ = 0.15)	29	3500	0.53	0.16
MNDA	50	92	0.79	0.17
15% *R*8	75	7	0.90	0.21
	100	2	1.09	0.19

random copolymer (ETBN), a straight line of negative slope was obtained when representing ln η_{cp} vs. $\bar{D}$. It is then interesting to verify if this empirical law is valid for different systems.

Table V shows values of viscosity at the cloud point (determined as discussed in the first part of the series[1]), and average diameters of dispersed phase particles, for different systems precured at several temperatures and containing various rubber amounts. Obviously, η_{cp} decreases with increasing temperature, and, as discussed in the first part,[1] it also decreases when increasing the rubber amount at a constant temperature (except for the sample containing 20% *R*).

Figure 11 shows the viscosity at the cloud point as a function of the average diameter of dispersed phase particles for different systems containing the same initial rubber amount and precured at several temperatures. For every system a distinct correlation is obtained. The fact that there is not a unique correlation for all of them, means that viscosity at the time of phase separation is not the only parameter affecting the morphology. Obviously, the miscibility of the thermoset with the particular rubber must play a significant role through the location of the metastable region in a conversion vs composition phase diagram.[29] A model for the phase separation process in these particular systems will be discussed in the following part of this series.

The differences between lines *a* and *b* in Figure 11 may reflect the different COOH content of both ETBNs or just slight variations in the acrylonitrile

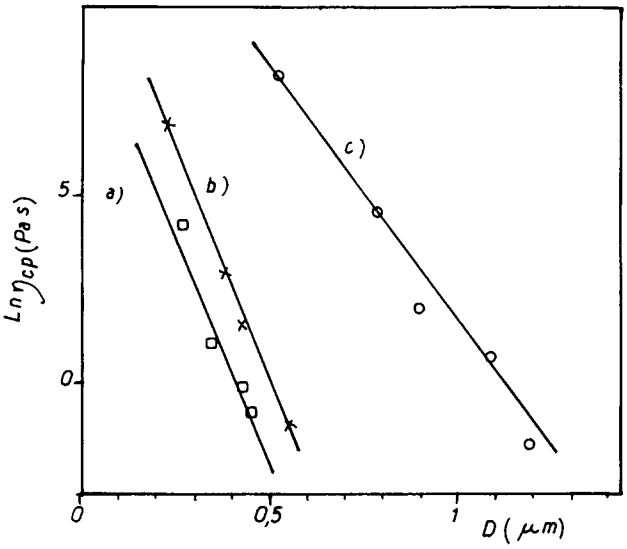

Figure 11 Viscosity at the cloud point vs. average diameter of dispersed phase particles for different systems cured at different temperatures: (a) DGEBA ($\bar{n}$ = 0.03)-3DCM—15% *R*8; (b) DGEBA ($\bar{n}$ = 0.03)-3DCM—15% *R*9; (c) DGEBA ($\bar{n}$ = 0.15)-MNDA—15% *R*8.

content. This last possibility explains the shift in the location of the straight line when a different batch of CTBN is used, as is shown in Figure 12.

Figure 13 shows the correlation for the particular system analyzed in this paper, including samples precured at several temperatures and containing different initial rubber concentrations. Only the sample with 20% *R* does not fit the correlation.

Figure 14 shows that a unique correlation may be

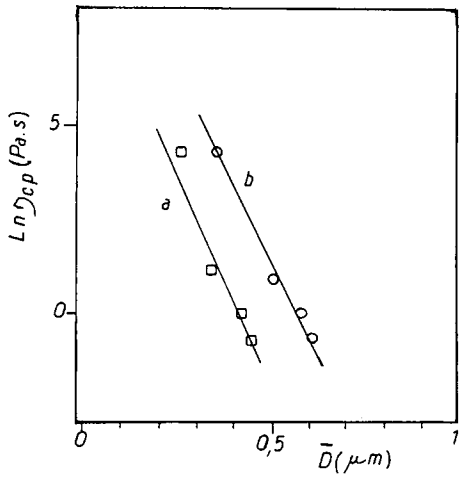

Figure 12 Viscosity at the cloud point vs. average diameter of dispersed phase particles for a single formulation DGEBA ($\bar{n}$ = 0.03)-3DCM—15% *R*8, prepared using two different batches of CTBN (a) and (b).

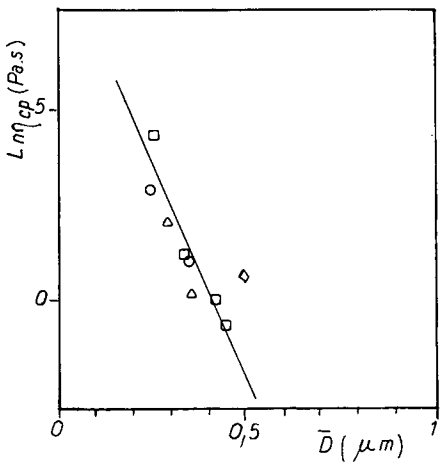

Figure 13 Viscosity at the cloud point vs. average diameter of dispersed phase particles for a system DGEBA (n = 0.03)-3DCM—variable % *R*8; (○) 6.5%; (△) 10.6%; (□) 15%; (◇) 20%.

obtained for every system by plotting the reduced viscosity vs. the reduced diameter, taking values at 29°C as a reference. The justification of this empiric correlation must be analyzed with great care because changes in temperature do not only affect phase separation rates, but also the thermodynamics of the mixture. These aspects will be discussed in the next part of this series.

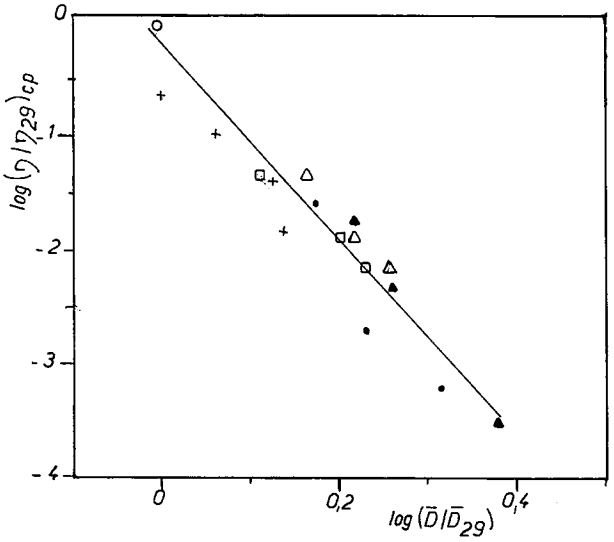

Figure 14 Reduced viscosity at the cloud point, ($\eta/\eta_{29°C}$), vs. reduced diameter ($\bar{D}/\bar{D}_{29°C}$) for every system: (▲): 6.5% and 10.6% *R*8; (■): 15% *R*8 (batch a); (◇): 15% *R*8 (batch b); (×): 15% *R*9; (●): DGEBA ($\bar{n}$ = 0.15)-MNDA—15% *R*8.

CONCLUSIONS

The influence of the cure schedule and initial rubber concentration on the morphologies generated in a DGEBA-based epoxy-3DCM-ETBN system, was discussed. The main conclusions from this study are:

- Morphological parameters determined by SEM are not affected by the type of fracture mode (tensile, flexural, and impact tests in a very broad range of strain rates).
- The average diameters measured by SEM are always higher than the corresponding values determined by TEM. While SEM gives the actual particle size distribution, TEM shows the distribution resulting from the random cut of dispersed domains during the microtoming of the sample.
- Increasing the cure temperature leads to an increase in the average size of dispersed domains. This is a general trend when the morphology is controlled by the phase separation rate rather than by the polymerization rate.
- Increasing the rubber amount leads to an increase in the average size of dispersed phase particles.
- The effective volume fraction of dispersed domains, as determined by SEM, increases significantly with the initial rubber concentration but does not depend very much on the cure temperature. Again, this supports the fact that morphology development is not controlled by the polymerization rate.
- The concentration of dispersed phase particles decreases with an increase in the cure temperature and does not show a significant variation with the initial rubber amount.
- The concentration of rubber dissolved in the matrix at the end of cure, increases with the initial rubber concentration but does not depend on cure temperature.
- Dispersed domains have a significant volume fraction of epoxy copolymer, i.e., close to 50%, for every formulation and cure cycle. A secondary phase separation takes place inside the dispersed particles. The rubbery phase relaxes at a lower temperature than pure rubber because of the presence of unrelaxed thermal stresses. The epoxy–amine phase segregated inside the particles relaxes at a very close—but lower—temperature than the matrix. This is ascribed to the presence of bonds between epoxy and CTBN moeities in dispersed domains and/or to a lower crosslink density of epoxy copolymer.
- A correlation between the viscosity at the cloud point and the average size of dispersed phase particles was found for every system independently of the cure temperature and the initial rubber amount (except for compositions close to the critical point). Different systems show different fittings indicating that other factors like the thermodynamic miscibility play a significant role in the phase separation process. A general correlation resulted when plotting the reduced viscosity at the cloud point vs. the reduced average size, taking values at 29°C as reference.

The contributions of F. Surivet (runs with R9) and J. F. Gérard (dynamic mechanical measurements) are gratefully acknowledged. This work was performed in the frame of a cooperation program between the National Research Councils of France (CNRS) and Argentina (CONICET).

REFERENCES

1. D. Verchère, H. Sautereau, J. P. Pascault, S. M. Moschiar, C. C. Riccardi, and R. J. J. Williams, *J. Appl. Polym. Sci.*, to appear.
2. C. K. Riew, E. H. Rowe, and A. R. Siebert, in *Toughness and Brittleness of Plastics*, ACS Symp. Ser. 154, R. D. Deanin and A. M. Crugnola, Eds., American Chemical Society, Washington DC, 1976, p. 326.
3. S. Kunz-Douglass, P. W. R. Beaumont, and M. F. Ashby, *J. Mater. Sci.*, **15**, 1109 (1980).
4. L. T. Manzione, J. K. Gillham, and C. A. McPherson, *J. Appl. Polym. Sci.*, **26**, 889 (1981).
5. L. T. Manzione, J. K. Gillham, and C. A. McPherson, *J. Appl. Polym. Sci.*, **26**, 907 (1981).
6. S. C. Kunz, J. A. Sayre, and R. A. Assink, *Polymer*, **23**, 1897 (1982).
7. L. C. Chan, J. K. Gillham, A. J. Kinloch, and S. J. Shaw, in *Rubber-Modified Thermoset Resins*, Adv. Chem. Ser. 208, C. K. Riew and J. K. Gillham, Eds., American Chemical Society, Washington DC, 1984, p. 235.
8. P. Bartlet, J. P. Pascault, and H. Sautereau, *J. Appl. Polym. Sci.*, **30**, 2955 (1985).
9. H. N. Naé, *J. Appl. Polym. Sci.*, **31**, 15 (1986).
10. E. Butta, G. Levita, A. Marchetti, and A. Lazzeri, *Polym. Eng. Sci.*, **26**, 63 (1986).
11. A. J. Kinloch and D. L. Hunston, *J. Mater. Sci. Lett.*, **6**, 131 (1987).
12. S. Montarnal, J. P. Pascault, and H. Sautereau, in *Rubber-Toughened Plastics*, Adv. Chem. Ser. 222, C. K. Riew, Ed., American Chemical Society, Washington DC, 1989, p. 193.

13. R. J. J. Williams, J. Borrajo, H. E. Adabbo, and A. J. Rojas, in *Rubber-Modified Thermoset Resins,* Adv. Chem. Ser. 208, C. K. Riew and J. K. Gillham, Eds., American Chemical Society, Washington DC, 1984, p. 195.
14. D. Verchère, H. Sautereau, J. P. Pascault, C. C. Riccardi, S. M. Moschiar, and R. J. J. Williams, *Macromolecules,* 725 (1990).
15. S. Hashemi and J. G. Williams, *J. Mater. Sci.,* **19,** 3746 (1984).
16. T. Takahama and P. H. Geil, *J. Polym. Sci. Polym. Phys. Ed.,* **20,** 1979 (1982).
17. Y. G. Lin, J. F. Gérard, J. Y. Cavaillé, H. Sautereau, and J. P. Pascault, *Polym. Bull.,* **17,** 97 (1987).
18. L. Holliday and G. Thackray, *Nature,* **201,** 270 (1964).
19. L. Holliday, in *Composite Materials,* L. Holliday, Ed., Elsevier, Amsterdam, 1966, p. 1.
20. E. E. Underwood, in *Quantitative Microscopy,* R. T. de Hoff and F. N. Rhines, Eds., McGraw-Hill, New York, 1968, p. 147.
21. A. J. Kinloch, C. A. Finch, and S. Hashemi, *Polym. Comm.,* **28,** 322 (1987).
22. S. D. Sjoerdsma, *Polym. Comm.,* **30,** 106 (1989).
23. S. Wu, *Polymer,* **26,** 1855 (1985).
24. T. G. Fox, *Bull. Am. Phys. Soc.,* **1,** 123 (1956).
25. C. B. Bucknall and T. Yoshii, *Br. Polym. J.,* **10,** 53 (1978).
26. W. A. Romanchik, J. E. Sohn, and J. F. Geibel, in *Epoxy Resin Chemistry II,* ACS Symp. Ser. 221, R. S. Bauer, Ed., American Chemical Society, Washington DC, 1983, p. 85.
27. E. J. Beckman, F. E. Karasz, R. S. Porter, W. J. McKnight, J. Van Hunsel, and R. Koningsveld, *Macromolecules,* **21,** 1193 (1988).
28. T. T. Wang and H. M. Zupko, *J. Appl. Polym. Sci.,* **26,** 2391 (1981).
29. A. Vazquez, A. J. Rojas, H. E. Adabbo, J. Borrajo, and R. J. J. Williams, *Polymer,* **28,** 1156 (1987).

Received March 3, 1990
Accepted April 17, 1990